Liquid Crystals
Publication details, including instructions for authors and subscription information:
http://www.informaworld.com/smpp/title~content=t713926090

New chlorine-substituted ferroelectric liquid crystals with four aromatic rings in the mesogenic core

V. Novotná; V. Hamplová; M. Kašpar; M. Glogarová

Online publication date: 11 November 2010

To cite this Article Novotná, V. , Hamplová, V. , Kašpar, M. and Glogarová, M.(2002) 'New chlorine-substituted ferroelectric liquid crystals with four aromatic rings in the mesogenic core', Liquid Crystals, 29: 11, 1435 — 1439
To link to this Article: DOI: 10.1080/0267829021000031234
URL: http://dx.doi.org/10.1080/0267829021000031234

LIQUID CRYSTALS, 2002, VOL. 29, NO. 11, 1435–1439

New chlorine-substituted ferroelectric liquid crystals with four aromatic rings in the mesogenic core

V. NOVOTNÁ*, V. HAMPLOVÁ, M. KAŠPAR, and M. GLOGAROVÁ

Institute of Physics, Academy of Sciences of the Czech Republic, Na Slovance 2, 182 21 Prague 8, Czech Republic

(*Received 22 April 2002; in final form 14 June 2002; accepted 24 July 2002*)

New series of liquid crystals with an alkyl-lactate chiral chain and four aromatic rings in the mesogenic core and chloro-substitution were synthesized. For all the compounds studied, SmA and SmC* phases, existing over very broad temperature ranges, were detected and characterized. Mesomorphic properties were analysed with respect to the lengths of the chiral and/or non-chiral chains.

1. Introduction

Liquid crystal materials with four aromatic rings in the mesogenic core have such high phase transition temperatures [1] that decomposition can occur near the clearing temperature. In our previous work [2] we studied the effect of chloro-substitution on the properties of ferroelectric liquid crystal materials containing four aromatic rings in the molecular core derived from 4-hydroxybiphenyl-4′-carboxylic acid and a lactate unit in the chiral chain. We found a decrease in the transition temperatures and a substantial increase in spontaneous polarization and spontaneous tilt angle in the chlorinated compounds. Recently, a relatively low clearing temperature (195°C) has been obtained by substitution of bromine at the same position in the four ring mesogenic core [3]. Moreover, this material exhibited both ferroelectric and antiferroelectric C phases.

Here we study the physical properties of series of ferroelectric liquid crystal materials laterally substituted by chlorine in the same core as that in ref. [2], with respect to the length of both the chiral and non-chiral chains. In contrast to ref. [3], where the asymmetric centre is derived from 2-octanol, in our new compounds the lactate unit is present in the chiral chain. The general formulae of the compounds studied are:

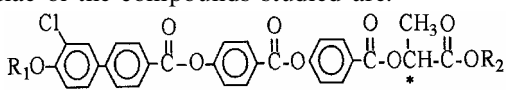

denoted FRCl *m*/*n*

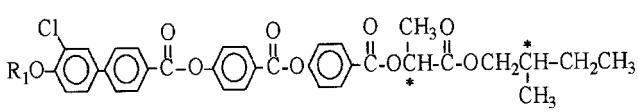

denoted FRCl *m*/**

Indices *m* and *n* show the number of carbon atoms in the R_1 and R_2 alkyl chains, respectively. The compounds FRCl *m*/** contain two chiral centres both with the (*S*) configuration.

2. Synthesis

The compounds were prepared following the scheme. The synthesis of intermediate compounds **4a** and **4b** has already been published in detail [4]. The lactates were esterified by protected 4-hydroxybenzoyl chloride **2**. In the next step the protecting group was removed by ammonolysis. The repeat reactions of phenols **3a** and **3b** with **2**, followed by ammonolysis, led to the compounds **4a** and **4b**, respectively, in 20–30% yield. The final products FRCl were prepared by the standard method of esterification with dicyclohexylcarbodiimide in presence of 4-*N*,*N*-dimethylaminopyridine in dichloromethane.

All crude products were chromatographed on silica gel (Kieselgel 60, Merck, Darmstadt) using a mixture of dichloromethane and ethanol (98:2) as eluent. After crystallization from ethanol the product purity was determined by HPLC, which was carried out with an Ecom high performance liquid chromatograph using a silica gel column Separon 7 μm, 3 × 150, Tessek with a mixture of toluene and methanol as eluent. The structures of all compounds were confirmed by ^{1}H NMR (200 MHz, $CDCl_3$, Varian, Gemini 2000).

3. Experimental

All measurements were performed on samples with the planar (book-shelf) geometry where the smectic layers are perpendicular to the confining glass plates. The 25 μm thick cells were filled in the isotropic phase by capillary action and consisted of glass plates coated with indium tin oxide (ITO) transparent electrodes having

* Author for correspondence; e-mail: novotna@fzu.cz

Liquid Crystals ISSN 0267-8292 print/ISSN 1366-5855 online © 2002 Taylor & Francis Ltd
http://www.tandf.co.uk/journals
DOI: 10.1080/0267829021000031234

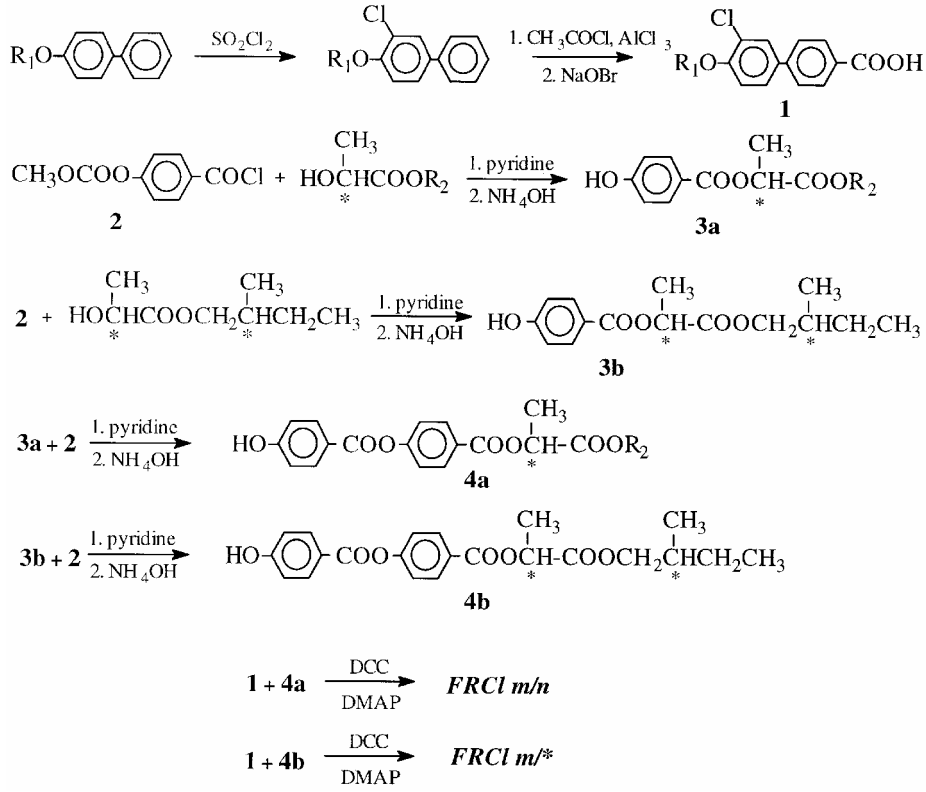

Scheme. Synthesis of the compounds studied. R_1 and R_2 are alkyl chains with m and n carbons, respectively.

the area $5 \times 5\,\mathrm{mm}^2$. Mesophases and phase transition temperatures were detected from the characteristic textures and texture changes observed by polarizing microscopy (Nikon E-600). For temperature control, a Linkam heating stage was used, which enabled temperature stabilization within ± 0.1 K. For several compounds, the phase transition temperatures were checked by differential scanning calorimetry (Pyris Diamond Perkin Elmer). During DSC measurements cooling and heating rates of $5\,\mathrm{K\,min}^{-1}$ were applied. The samples were placed in a nitrogen atmosphere and hermetically sealed in aluminium pans. The mass of the samples was about 6 mg.

The spontaneous polarization, $\mathbf{P}_s$, was determined from the $P(E)$ hysteresis loop measured by the Sawyer–Tower method at a frequency of 50 Hz. The spontaneous tilt, θ_s, was determined from the angle difference between minimum transmission (extinction) positions between crossed polarizers measured under opposite d.c. electric fields (about $40\,\mathrm{kV\,cm}^{-1}$). The helicoidal pitch, p, was obtained from the diffraction of He-Ne laser light on the dechiralization lines which exist in planar samples due to the strong polar anchoring at the surfaces.

A memory oscilloscope leCroy 9304 provided information from the switching current peak on the time axis. The position of the peak represents the switching time, τ. The frequency dispersion of the complex permittivity $\varepsilon^*(\omega) = \varepsilon' - \mathrm{i}\varepsilon''$ was measured using a Schlumberger impedance analyser in the frequency range 10 Hz–1 MHz. During the frequency sweeps, the temperature was kept stable within ± 0.1 K.

4. Results

The sequences of phases and phase transition temperatures determined from the texture observations are shown in the table. All compounds exhibit very wide temperature ranges of the SmA and SmC* phases. The SmA–SmC phase transition could be recognized by the appearance of the dechiralization lines. The SmC* phase may be obtained partially monotropic due to supercooling. For all the materials the sample alignment gradually deteriorates on cooling below approximately 50°C, but no crystallization occurs down to a temperature of −50°C. On subsequent heating a recrystallization occurs, which is seen as a negative peak in the DSC traces (see figure 1).

Typical temperature dependences of $\mathbf{P}_s$ and θ_s are shown in figures 2(*a*) and 2(*b*), respectively, for compounds differing in the number of carbon atoms in the chiral chain and with a constant number of carbons in the non-chiral chain ($m = 6$). The values of $\mathbf{P}_s$ increase on cooling within the whole SmC* phase range; the θ_s values tend to saturate at low temperatures. Under the electric field used for the measurements ($40\,\mathrm{kV\,cm}^{-1}$),

Table. Phases and transition temperatures for the compounds studied; m.p. is the melting point. The spontaneous polarization, $\mathbf{P}_s$, was measured at 50°C below the SmA–SmC* phase transition.

Compound	m.p.	SmC*		SmA		I	$\mathbf{P}_s$ nC cm^{-2}
FRCl 6/5	79	•	134	•	231	•	116
FRCl 7/5	71	•	152	•	221	•	120
FRCl 8/5	69	•	163	•	219	•	119
FRCl 9/5	85	•	164	•	215	•	115
FRCl 6/6	95	•	129	•	229	•	124
FRCl 7/6	89	•	145	•	219	•	114
FRC; 8/6	85	•	161	•	216	•	98
FRCl 9/6	75	•	163	•	208	•	103
FRCl 6/10	86	•	99	•	216	•	110
FRCl 7/10	87	•	124	•	205	•	113
FRCl 6/**	70	•	142	•	224	•	103
FRCl 7/**	92	•	152	•	223	•	124
FRCl 8/**	88	•	165	•	210	•	159

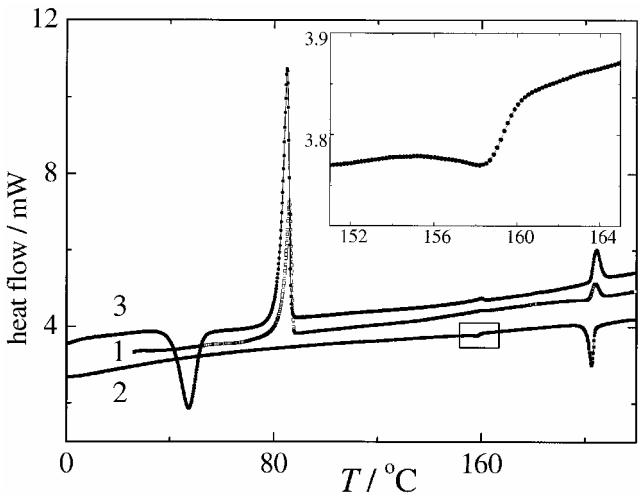

Figure 1. DSC traces for FRCl 8/*. Numbers 1, 2 and 3 denote first heating of the virgin sample, cooling to a temperature of −50°C and the subsequent heating run, respectively. The inset shows on an enlarged scale the SmA–SmC* phase transition taken on cooling.

crystallization occurs at about 40°C for all the materials in spite of the fact that this cannot be achieved on cooling without a field. The values of $\mathbf{P}_s$ measured at 50°C below the SmA–SmC* phase transition temperature, T_c, are shown in the table. The values of θ_s taken at 50°C below T_c are shown in figure 3. For a fixed length of the chiral chain (n), the tilt angle essentially increases with increasing length of the non-chiral chain (m), while the dependence on n is not regular.

The typical temperature dependence of the pitch length is shown in figure 4 for the compounds with $m = 6$. It was found that the pitch is practically independent of the length of the non-chiral chain characterized by m, but increases with the length of the chiral chain denoted by n (see figure 4). The pitch is shortest for materials with two chiral centres, probably due to the very high rotatory power of the strongly chiral molecules. The temperature dependences of the pitch length taken on cooling exhibit a steep increase just below the SmA–SmC* phase transition and then become constant over the whole measured temperature range. At temperatures below 50°C the pitch cannot be detected because the diffraction rings are smeared out. This is connected with deterioration of the texture as mentioned above.

Switching properties in the SmC* phase were studied using a square wave electric field by measuring the current density as a function of time. In figure 5 the switching time τ, evaluated as a time delay between the pulse edge and the current peak, is shown as a function of temperature for compounds with two chiral centres. The τ values increase from values of tens of microseconds below T_c to values of several milliseconds when approaching 40°C on cooling.

Dielectric spectra exhibit one relaxation in both the SmA and SmC* phases. Spectra were analysed using the Cole–Cole formula for the frequency-dependent complex permittivity $\varepsilon^*(f)$

$$\varepsilon^* - \varepsilon_\infty = \frac{\Delta\varepsilon}{1 + (\mathrm{i}f/f_r)^{(1-\alpha)}} - \mathrm{i}\frac{\sigma}{2\pi\varepsilon_0 f}$$

where f_r is the relaxation frequency, $\Delta\varepsilon$ is the dielectric strength of the mode, α is the distribution parameter, σ is the conductivity, ε_∞ is the high frequency permittivity, and ε_0 is the permittivity of a vacuum. All parameters were determined by simultaneous fitting of both real and imaginary parts of the complex permittivity $\varepsilon^*(f)$ to the experimental data. Temperature dependences of the fitted f_r and $\Delta\varepsilon$ are shown for FRCl 6/10 in figure 6. For the other compounds the results were similar. The

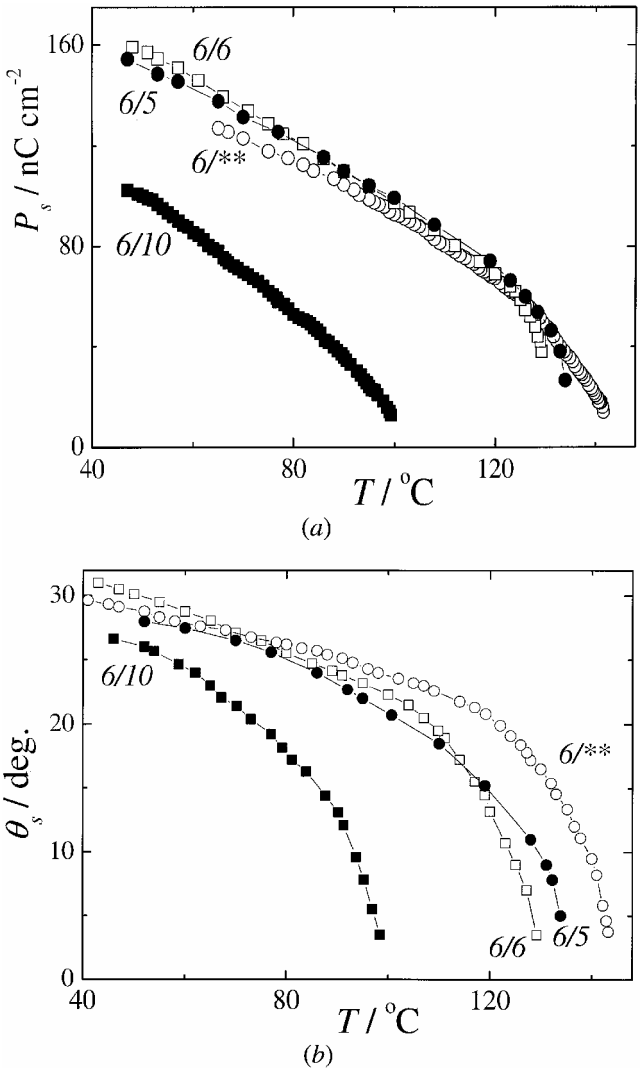

Figure 2. Temperature dependences of (*a*) spontaneous polarisation and (*b*) spontaneous tilt angle for the compounds indicated and having the same length of non-chiral chain ($m = 6$). Compounds are denoted by m/n, and $n = **$ denotes the chain with two chiral centres.

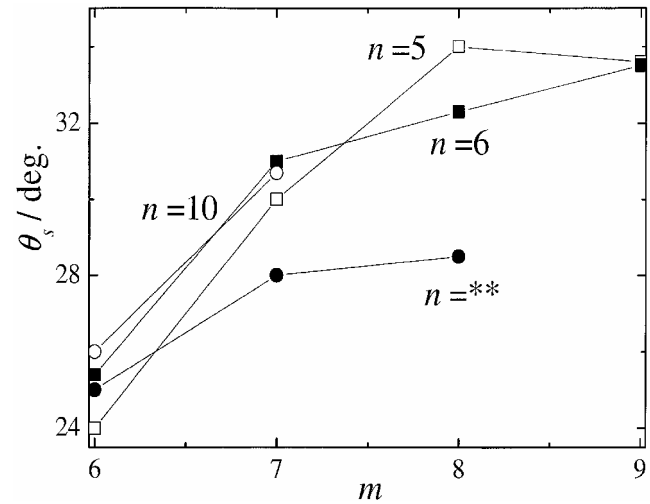

Figure 3. Spontaneous tilt angle, θ_s, taken at 50°C below the SmA–SmC* phase transition versus the number of carbon atoms in the chiral chain (m). For each curve the length of the chiral chain (n) is fixed.

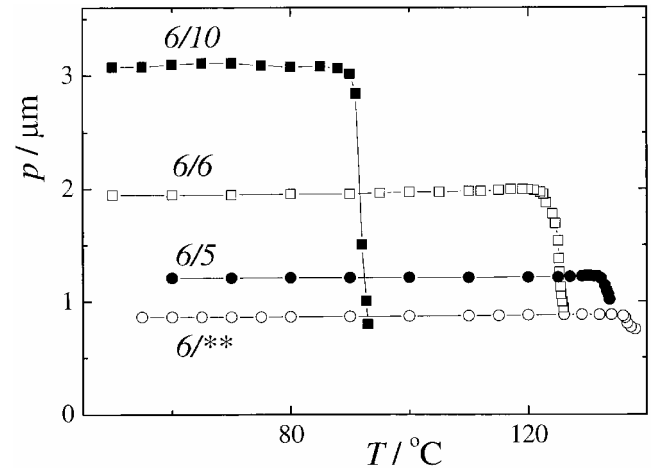

Figure 4. Temperature dependence of the helicoidal pitch, p, for materials with $m = 6$.

value of parameter α is about 0.1, which gives evidence for the nearly monodispersive character of the relaxation, except for the temperature range less than 1 K just below T_c, where $\alpha \approx 0.2$.

5. Discussion and conclusions

The compounds studied from the new series with four phenyl rings in the mesogenic core, one being substituted with chlorine, exhibit wide range SmA and SmC* phases. The antiferroelectric phase does not occur in these materials. On the other hand, a similar compound substituted by bromine [3] exhibited the SmC^*_A phase. A possible explanation is that the lactate group present in the chiral chain of the chloro-materials might prevent anticlinic order.

The transition between the SmA and SmC* phases seems to be second order. This conclusion is derived from the DSC plots (see figure 1), which show no latent heat and the absence of thermal hysteresis, and is supported by the temperature dependences of the spontaneous polarization and tilt angle which exhibit no visible jumps at this transition.

The SmC* phase while persisting down to ≈ -50°C on cooling is then monotropic. In the metastable temperature range, the switching time steeply increases with lowering temperature (figure 5). Simultaneously the sample texture deteriorates, which becomes more noticeable below 50°C. These findings indicate a gradual 'solidification' of the SmC* phase to a glassy state. For

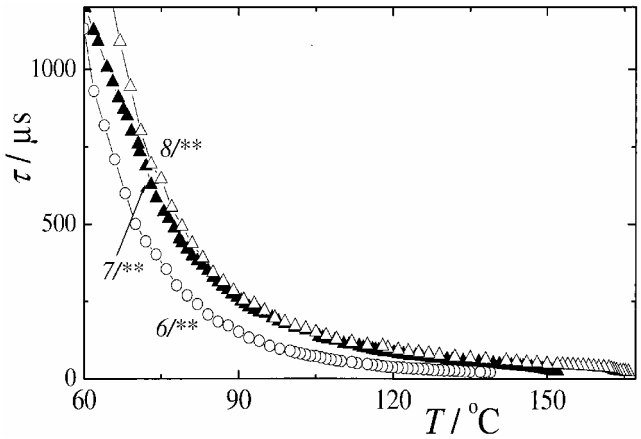

Figure 5. Temperature dependence of the switching time, τ, for materials with two chiral centres.

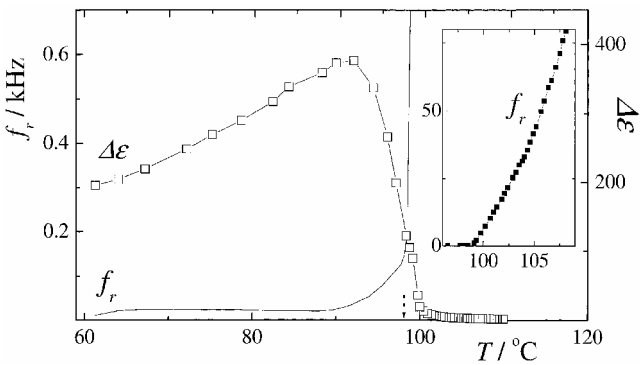

Figure 6. Temperature dependence of the relaxation frequency, f_r, and the dielectric strength, $\Delta\varepsilon$, obtained from fitting of dielectric spectroscopy data for FRCl 6/10. The arrow indicates the SmA–SmC* phase transition temperature. In the inset $f_r(T)$ is shown on an enlarged scale.

all the materials, recrystallization occurs at about 40°C on subsequent heating (see figure 1).

As for the effect of the lengths of the chiral (n) and non-chiral (m) chains on the basic characteristics of the SmC* phase, one can note the following tendencies. The tilt angle increases with increasing m (figure 3). On the other hand, the value of p is driven by the properties of the chiral chain only. It increases with n, being lowest for the compounds with two chiral centres in the end chain. The other dependences are not regular.

The dielectric spectroscopy shows a soft mode in the SmA phase. The relaxation frequency of this mode exhibits a linear decrease when approaching the SmA–SmC* phase transition (see inset in figure 6). In the SmC* phase, the Goldstone mode contributes to the permittivity except in the close vicinity of the phase transition to the SmC* phase, where the Goldstone mode may be mixed with the weak soft mode. The coexistence of both modes is indicated by the increase of the parameter α up to 0.2. The dielectric strength $\Delta\varepsilon$ of the Goldstone mode is much higher than that of the soft mode and can be expressed [5] as:

$$\Delta\varepsilon \cong \frac{1}{K}\left(\frac{p\mathbf{P}_s}{\theta_s}\right)^2$$

where K is the twist elastic constant. The increase of $\Delta\varepsilon$ just below the SmA–SmC* phase transition can be explained by the abrupt increase of p (see figure 4). The subsequent decrease of $\Delta\varepsilon$ on cooling may be connected with the increase in the K value due to gradual freezing of the SmC* phase to a glassy state.

The authors thank to Dr P. Vaněk and Mrs Y. Lhotáková from the Institute of Physics, Academy of Sciences of the Czech Republic for help with the DSC measurements. This work was supported by grants No. 202/02/0840 and 106/00/0580 from the Grant Agency of the Czech Republic.

References

[1] Chen, J.R.-H., Hsiue, G.-H., Hwang, C.-P., and Wu, J.-L., 1995, *Liq. Cryst.*, **19,** 803.
[2] Hamplová, V., Kašpar, M., Novotná, V., and Glogarová, M., 2002, *Ferroelectrics*, **276,** 57.
[3] Gisse, P., Cluzeau, P., Ravaine, V., and Nguyen, H. T., 2002, *Liq. Cryst.*, **29,** 91.
[4] Bubnov, A., Hamplová, V., Kašpar, M., Glogarová, M., and Vaněk, P., 2000, *Ferroelectrics*, **243,** 27.
[5] Levstik, A., Carlsson, T., Filipič, C., and Žekš, B., 1987, *Phys. Rev. A,* **35,** 3527.